Supporting information

Mixed-metal metallocavitands: A new approach to tune their electrostatic potentials for controllable selectivity towards substituted benzene derivatives

Jian-Jun Liu,[a] Ying-Fang Guan,[a] Yong Chen,[a] Mei-Jin Lin,[ab*] Chang-Cang Huang [a*] and Wen-Xin Dai[a]

[a] *State Key Laboratory of Photocatalysis on Energy and Environment, College of Chemistry, Fuzhou University, China, 350116; and* [b] *State Key Laboratory of Structural Chemistry, Fujian Institute of Research on the Structure of Matter, CAS, China, 350002. Email: meijin_lin@fzu.edu.cn, cchuang@fzu.edu.cn, Tel: 0086 591 2286 6143*

Table of Contents:

1. Experimental Details and Synthesis

Materials and measurements: Zinc acetylacetonate (98%), copper acetate (analytical reagent grade), benzoyl chloride (analytical reagent grade), potassium thiocyanate (analytical reagent grade), *p*-chlorophenoxyacetic acid (≥99%), and hydrazine hydrate (85%), *N*, *N*-dimethylacetamide (DMA, analytical reagent grade), dimethyl sulfoxide (DMSO, analytical reagent grade), chloroform (analytical reagent grade), chlorobenzene (analytical reagent grade), bromobenzene (analytical reagent grade), iodobenzene (analytical reagent grade), toluene (analytical reagent grade) and aniline (analytical reagent grade) were obtained from commercial suppliers. All chemicals and reagents were used as received unless otherwise stated. NMR spectra were recorded with a Bruker Avance 400 MHz NMR spectrometer. Chemical shifts are given in parts per million (ppm) and referred to TMS as internal standard. ^{1}H coupling constants *J* are given in Hertz (Hz). Flourier transformation infrared (FTIR) spectra were recorded from KBr discs on a Perkin-Elmer Spectrum 2000 FT-IR spectrometer. Powder X-ray diffraction (PXRD) patterns were recorded with a Rigaku MiniFlex-II X-Ray diffractometer with Cu Kα radiation (λ = 1.54178 Å) and high-resolution mass spectrum were recorded on a Thermo Fisher Scientific Exactive Plus system. Elemental analyses for Cu and Zn were obtained using Inductively Coupled Plasma OES spectrometer.

Synthesis: H_2L was prepared according to the literature method [S1].

Synthesis of M_8L_8: $Cu(oAc)_2{\cdot}2H_2O$ (40.0 mg, 0.2 mmol) and H_2L (72.4 mg, 0.2 mmol) were dissolved in DMA/$CHCl_3$ (1/1, v/v, 10mL), then the solution was stirred for 2 h at room temperature. The resulting black solution was filtered. After standing for several days, black cubic crystals were obtained from the filtrate. Yield, 68% based on Cu. IR (KBr disk, υ cm^{-1}): 3334 (m), 3280 (w), 3038 (w), 1673(s), 1558(s), 1439 (s), 1412 (m), 1245(m), 1065(m), 815 (s), 677 (m), 647(m), 470(m). HRMS (ESI-) *m/z* calculated for $C_{128}H_{96}Cl_8Cu_8N_{24}O_{24}S_8$: 3402.69; found 3401.63.

Synthesis of $[Zn_{1-x}Cu_x]_8L_8$ (x = 0.05, 0.10, 0.15, 0.20, 0.25, 0.30 and 0.35): Mixed-metal complexes were prepared by using varying amounts of metal salts (zinc acetylacetonate and copper acetate) combined with H_2L. The solid reagents were then dissolved in DMA/$CHCl_3$ (1/1 v/v) and was stirred for 2 h at room temperature. The resulting black solution was filtered. After standing for several days, black crystals were obtained from the filtrate. Analyses of the relative molar concentration of the Cu and Zn are consistent with the corresponding ratios in the starting mixture according to ICP (Table S8).

2. X-ray Diffraction Analysis

Suitable single crystals of Cu_8L_8 and $[Zn_{1-x}Cu_x]_8L_8$ (x = 0.10, 0.25, 0.35) were mounted on glass fibers for the X-ray measurement. Diffraction data were collected on a Rigaku-AFC7 equipped with a Rigaku Saturn CCD area-detector system. The measurement was made by using graphic monochromatic Mo Kα radiation (λ= 0.71073 Å) at 113 K under a cold nitrogen stream. The frame data were integrated and absorption correction using a Rigaku *CrystalClear* program package. All calculations were performed with the *SHELXTL-97* program package [S2], and structures were solved by direct methods and refined by full-matrix least-squares against F^2. All non-hydrogen atoms except for the disordered moieties were refined anisotropically, and hydrogen atoms of the organic ligands were generated theoretically onto the specific atoms and refined isotropically with fixed thermal factors. The diffraction data were treated by the "SQUEEZE" method as implemented in PLATON[S3] to remove diffuse electron density associated with these badly disordered solvent molecules. In the mixed-metal complexes, due to the nearly electron density of Cu and Zn, it is hard to distinguish them according to X-ray single-crystal diffraction. In the structure of $[Zn_{1-x}Cu_x]_8L_8$ (x = 0.10, 0.25), uniformly use Zn for calculation to obtain lower R1 value than use Cu. However, in the case of $[Zn_{1-x}Cu_x]_8L_8$ (x = 35%), use Cu for calculation to obtain lower R1 value than use Zn. In order to obtain lower R1 value, we use Zn to calculation for $[Zn_{1-x}Cu_x]_8L_8$ (x = 0.10, 0.25), use Cu to calculation for $[Zn_{1-x}Cu_x]_8L_8$ (x = 0.35). We can infer that there are about 0.78, 2.00 and 3.16 Cu on average per formula unit for $[Zn_{1-x}Cu_x]_8L_8$ (x = 0.10, 0.25, 0.35) based on ICP analysis, respectively (Table S8). Crystal data and refinement conditions are presented Table S1. Crystallographic data have been deposited with the Cambridge Crystallographic Data Center with reference number CCDC 1021744-1021747 for $[Zn_{1-x}Cu_x]_8L_8$ (x = 0.10, 0.25, 0.35) and Cu_8L_8. These data can be obtained free of charge from The Cambridge Crystallographic Data Centre *via* www.ccdc.cam.ac.uk/data_request/cif.

Table S1. Crystal data and structure refinement parameters

Complexes	**Cu_8L_8**	**$[Zn_{1-x}Cu_x]_8L_8$ (x = 0.10)**	**$[Zn_{1-x}Cu_x]_8L_8$ (x = 0.25)**	**$[Zn_{1-x}Cu_x]_8L_8$ (x = 0.35)**
Crystal size (mm)	0.44 x 0.19 x 0.18	0.48 x 0.42 x 0.08	0.42 x 0.30 x 0.07	0.45 x 0.27 x 0.24
Empirical Formula	$C_{166}H_{181.5}Cl_8Cu_8N_{33.5}O_{33.5}S_8$	$C_{180}H_{213}C_{18}Cu_{0.78}N_{37}O_{37}S_8Zn_{7.22}$	$C_{192}H_{240}Cl_8Cu_2N_{40}O_{40}S_8Zn_6$	$C_{158}H_{161.5}Cl_8Cu_{3.16}N_{31.5}O_{31.5}S_8Zn_{4.84}$
Formula weight	4230.35	4548.49	4807.62	4062.94
Crystal system	Monoclinic	Triclinic	Triclinic	Monoclinic
Space group	*C*2/c	$P\bar{1}$	$P\bar{1}$	*C*2/c
***a* (Å)**	37.385(8)	18.852(4)	18.813(4)	42.385(9)
***b* (Å)**	14.229(3)	19.026(4)	18.842(4)	19.464(4)
***c* (Å)**	36.842(7)	31.163(6)	31.129(6)	26.821(5)
***α* (°)**	90	96.31(3)	96.26(3)	90
***β* (°)**	109.73(3)	101.99(3)	101.21(3)	118.36(3)
***γ* (°)**	90	90.83(3)	90.80(3)	90
***V* (Å^3)**	18448(6)	10860(4)	10753(4)	19471(7)
Z	4	2	2	4
***Dc* (g/ cm^3)**	1.523	1.391	1.485	1.386
μ(Mo K*α*) (mm^{-1})	1.190	1.108	1.109	1.191
***F*(000)**	8704	4702	4988	8331
Collected reflections	71645	92354	90552	80459
Independent reflections	20898 (0.0990)	48022 (0.0774)	47278 (0.0857)	22293 (0.0775)
Goodness-of-fit on F^2	1.043	1.007	1.007	1.238
R_1^a, wR_2^b ($I>2\sigma(I)$)	0.0833, 0.2141	0.0814, 0.2225	0.0890, 0.2375	0.1400, 0.4177
R_1^a, wR_2^b (all data)	0.1120, 0.2336	0.1156, 0.2441	0.1274, 0.2612	0.1679, 0.4532

Table S2. Unit cell parameters of Zn_8L_8, Cu_8L_8 and $[Zn_{1-x}Cu_x]_8L_8$ (x = 0.05, 0.10, 0.15, 0.20, 0.25, 0.30 and 0.35)

Complex	*a* (Å)	*b* (Å)	*c* (Å)	*α* (°)	*β* (°)	*γ* (°)	*V* (Å^3)	Space Group
Zn_8L_8	18.823(4)	19.042(4)	31.313(6)	96.46(3)	102.02(3)	90.42(3)	10902(4)	$P\bar{1}$
$[Zn_{1-x}Cu_x]_8L_8$ (x = 0.05)	18.907(4)	19.102(4)	30.995(6)	96.36(3)	102.03(3)	90.76(3)	10873(4)	$P\bar{1}$
$[Zn_{1-x}Cu_x]_8L_8$ (x = 0.10)	18.852(4)	19.026(4)	31.163(6)	96.31(3)	101.99(3)	90.83(3)	10860(4)	$P\bar{1}$
$[Zn_{1-x}Cu_x]_8L_8$ (x = 0.15)	18.911(4)	19.157(4)	31.240(6)	96.37(3)	102.24(3)	90.93(3)	11093(4)	$P\bar{1}$
$[Zn_{1-x}Cu_x]_8L_8$ (x = 0.20)	18.836(4)	19.072(4)	31.724(4)	97.02(3)	106.72(3)	90.25(3)	11084(4)	$P\bar{1}$
$[Zn_{1-x}Cu_x]_8L_8$ (x = 0.25)	18.813(4)	18.842(4)	31.129(6)	96.26(3)	101.21(3)	90.80(3)	10753(4)	$P\bar{1}$
$[Zn_{1-x}Cu_x]_8L_8$ (x = 0.30)	42.334(9)	19.478(4)	26.785(5)	90.00	118.55(3)	90.00	19401(7)	*C*2/*c*
$[Zn_{1-x}Cu_x]_8L_8$ (x = 0.35)	42.385(9)	19.464(4)	26.821(5)	90.00	118.36(3)	90.00	19471(7)	*C*2/*c*
Cu_8L_8	37.385(8)	14.229(3)	36.842(7)	90.00	109.73(3)	90.00	18448(6)	*C*2/*c*

Table S3. Unit cell parameters of as-synthesized crystals obtained from PhXs. $[Zn_{1-x}Cu_x]_8L_8$ (x = 0.05)

Complex	$[Zn_{1-x}Cu_x]_8L_8$ (x = 0.05)+PhCl	$[Zn_{1-x}Cu_x]_8L_8$ (x = 0.05)+PhBr	$[Zn_{1-x}Cu_x]_8L_8$ (x = 0.05)+PhI	$[Zn_{1-x}Cu_x]_8L_8$ (x = 0.05)+$PhCH_3$	$[Zn_{1-x}Cu_x]_8L_8$ (x = 0.05)+$PhNH_2$
***a* (Å)**	19.631 (4)	19.652(4)	19.443(4)	19.636(4)	19.587(4)
***b* (Å)**	30.961(6)	31.267(6)	31.367(6)	30.964(6)	31.029(6)
***c* (Å)**	18.383(4)	18.715(4)	18.675(4)	18.632(4)	18.836(4)
***α* (°)**	90.00	90.00	90.00	90.00	90.00
***β* (°)**	90.00	90.00	90.00	90.00	90.00
***γ* (°)**	90.00	90.00	90.00	90.00	90.00
***V* (Å^3)**	11173(4)	11493	11343(4)	11321	11385
Space Group	*P*ban	*P*ban	*P*ban	*P*ban	*P*ban

Table S4. Unit cell parameters of as-synthesized crystals obtained from PhXs. $[Zn_{1-x}Cu_x]_8L_8$ (x = 0.10)

Complex	$[Zn_{1-x}Cu_x]_8L_8$ (x = 0.10)+PhCl	$[Zn_{1-x}Cu_x]_8L_8$ (x = 0.10)+PhBr	$[Zn_{1-x}Cu_x]_8L_8$ (x = 0.10)+PhI	$[Zn_{1-x}Cu_x]_8L_8$ (x = 0.10)+$PhCH_3$	$[Zn_{1-x}Cu_x]_8L_8$ (x = 0.10)+$PhNH_2$
***a* (Å)**	18.843(4)	19.516(4)	19.373(4)	19.535(4)	19.652(4)
***b* (Å)**	19.026(4)	30.956(6)	31.094(6)	30.985(6)	31.262(6)
***c* (Å)**	31.156(6)	18.305(4)	18.784(4)	18.324(4)	18.714(4)
***α* (°)**	96.32(3)	90.00	90.00	90.00	90.00
***β* (°)**	101.98(3)	90.00	90.00	90.00	90.00
***γ* (°)**	90.85(3)	90.00	90.00	90.00	90.00
***V* (Å^3)**	10858(4)	11059(4)	10868(4)	11052(4)	11493(4)
Space Group	$P\bar{1}$	*P*ban	*P*ban	*P*ban	*P*ban

Table S5. Unit cell parameters of as-synthesized crystals obtained from PhXs. $[Zn_{1-x}Cu_x]_8L_8$ (x = 0.15)

Complex	$[Zn_{1-x}Cu_x]_8L_8$ (x = 0.15)+PhCl	$[Zn_{1-x}Cu_x]_8L_8$ (x = 0.15)+PhBr	$[Zn_{1-x}Cu_x]_8L_8$ (x = 0.15)+PhI	$[Zn_{1-x}Cu_x]_8L_8$ (x = 0.15)+$PhCH_3$	$[Zn_{1-x}Cu_x]_8L_8$ (x = 0.15)+$PhNH_2$
***a* (Å)**	18.982(4)	19.632(4)	19.533(4)	19.422(4)	19.602(4)
***b* (Å)**	19.115(4)	30.968(6)	30.935(6)	31.172(6)	30.974(6)
***c* (Å)**	31.303(6)	18.634(4)	18.394(4)	18.836(4)	18.256(4)
***α* (°)**	96.12(3)	90.00	90.00	90.00	90.00
***β* (°)**	102.25(3)	90.00	90.00	90.00	90.00
***γ* (°)**	90.73(3)	90.00	90.00	90.00	90.00
***V* (Å^3)**	11021(4)	11321(4)	11114(4)	11403(4)	11084(4)
Space Group	$P\bar{1}$	*P*ban	*P*ban	*P*ban	*P*ban

Table S6. Unit cell parameters of as-synthesized crystals obtained from PhXs. $[Zn_{1-x}Cu_x]_8L_8$ (x = 0.20)

Complex	$[Zn_{1-x}Cu_x]_8L_8$ (x = 0.20)+PhCl	$[Zn_{1-x}Cu_x]_8L_8$ (x = 0.20)+PhBr	$[Zn_{1-x}Cu_x]_8L_8$ (x = 0.20)+PhI	$[Zn_{1-x}Cu_x]_8L_8$ (x = 0.20)+$PhCH_3$	$[Zn_{1-x}Cu_x]_8L_8$ (x = 0.20)+$PhNH_2$
***a* (Å)**	18.925(4)	19.604(4)	19.586(4)	19.355(4)	19.185(4)
***b* (Å)**	19.064(4)	31.123(6)	30.987(6)	30.974(6)	31.662(6)
***c* (Å)**	31.143(6)	18.445(4)	18.832(4)	18.838(4)	19.072(4)
***α* (°)**	96.45(3)	90.00	90.00	90.00	90.00
***β* (°)**	102.62(3)	90.00	90.00	90.00	90.00
***γ* (°)**	90.84(3)	90.00	90.00	90.00	90.00
***V* (Å³)**	10886(4)	11253(4)	11429(4)	11293(4)	11585(4)
Space Group	$P\bar{1}$	*P*ban	*P*ban	*P*ban	*P*ban

Table S7. Unit cell parameters of as-synthesized crystals obtained from PhXs. $[Zn_{1-x}Cu_x]_8L_8$ (x = 0.25)

Complex	$[Zn_{1-x}Cu_x]_8L_8$ (x = 0.25)+PhCl	$[Zn_{1-x}Cu_x]_8L_8$ (x = 0.25)+PhBr	$[Zn_{1-x}Cu_x]_8L_8$ (x = 0.25)+PhI	$[Zn_{1-x}Cu_x]_8L_8$ (x = 0.25)+$PhCH_3$	$[Zn_{1-x}Cu_x]_8L_8$ (x = 0.25)+$PhNH_2$
***a* (Å)**	19.134(4)	19.092(4)	18.938(4)	18.956(4)	19.172(4)
***b* (Å)**	19.198(4)	19.235(4)	19.068(4)	18.969(4)	19.215(4)
***c* (Å)**	31.862(6)	31.403(6)	31.142(6)	30.973(6)	31.534(6)
***α* (°)**	97.86(3)	96.64(3)	96.41(3)	96.31(3)	97.05(3)
***β* (°)**	102.96(3)	102.57(3)	102.60(3)	101.56(3)	102.74(3)
***γ* (°)**	90.31(3)	90.90(3)	90.93(3)	90.84(3)	90.65(3)
***V* (Å³)**	11365(4)	11163(4)	10886(4)	11086(4)	11425(4)
Space Group	$P\bar{1}$	$P\bar{1}$	$P\bar{1}$	$P\bar{1}$	$P\bar{1}$

3. ^{1}H NMR Spectra

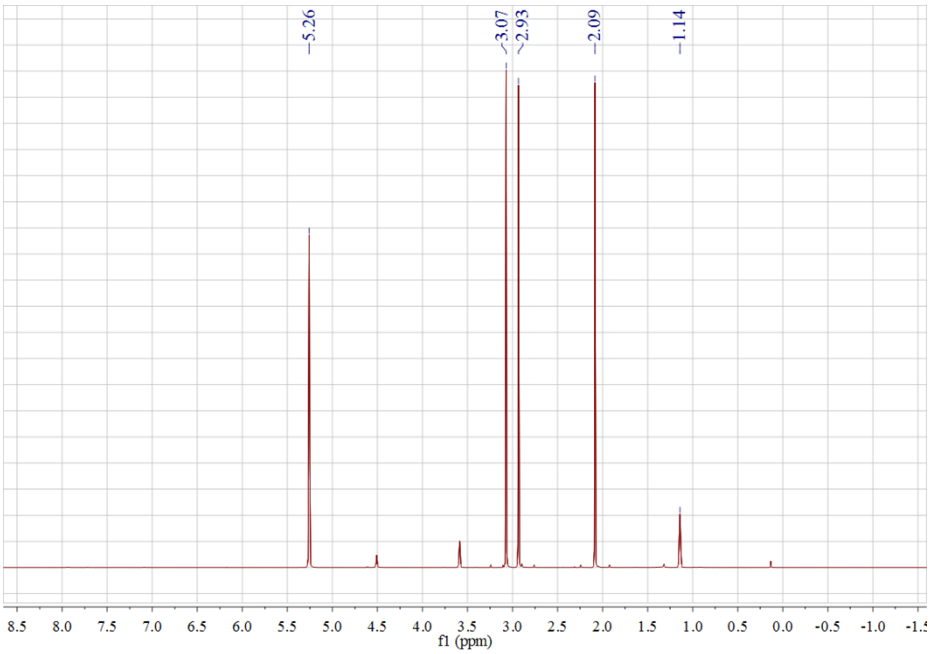

Figure S1. The ^{1}H NMR spectra of PhCl that is extracted from as-synthesized $[Zn_{1-x}Cu_x]_8L_8$ (x = 0.10) crystals obtained from PhCl (400 MHz, EtOD, 293 K). It is worth noting that the ^{1}H NMR spectra results, the peak of PhCl can't be observed in 8-7 ppm, which indicated that no any PhCl was included, while the peak 3.08, 2.94, and 2.09 ppm is DMA molecules from crystals. In addition, 5.26, 3.59 and 1.14 ppm assigned to the EtOH of EtOD.

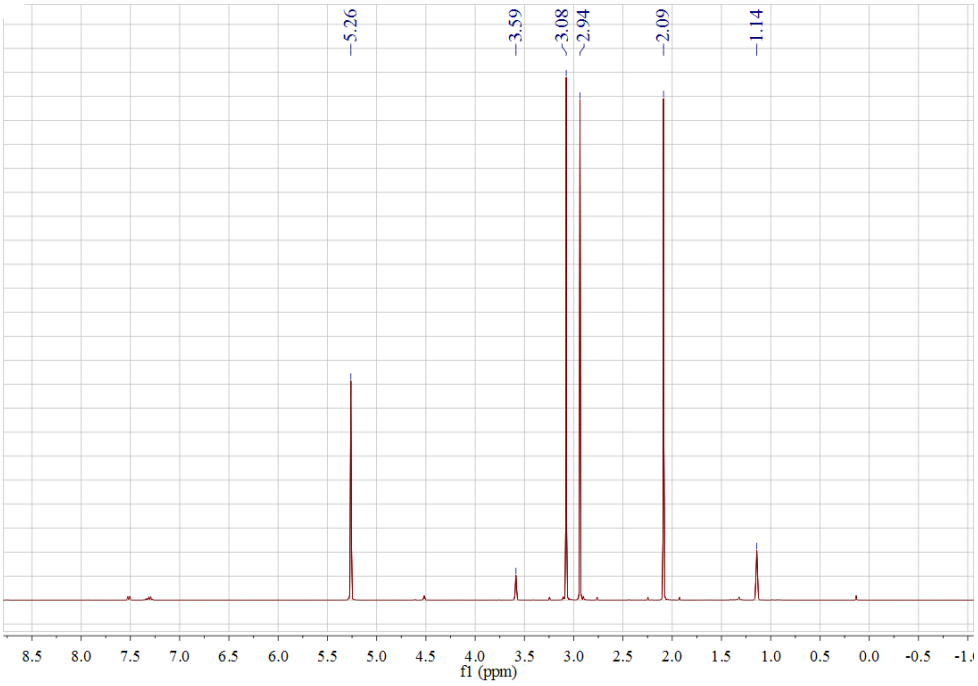

Figure S2. The ^{1}H NMR spectra of PhBr that is extracted from as-synthesized $[Zn_{1-x}Cu_x]_8L_8$ (x = 0.25) crystals obtained from PhBr (400 MHz, EtOD, 293 K). The peak of PhBr very weak in 8-7ppm, which indicated that $[Zn_{1-x}Cu_x]_8L_8$ (x = 0.25) almost not contain PhBr.

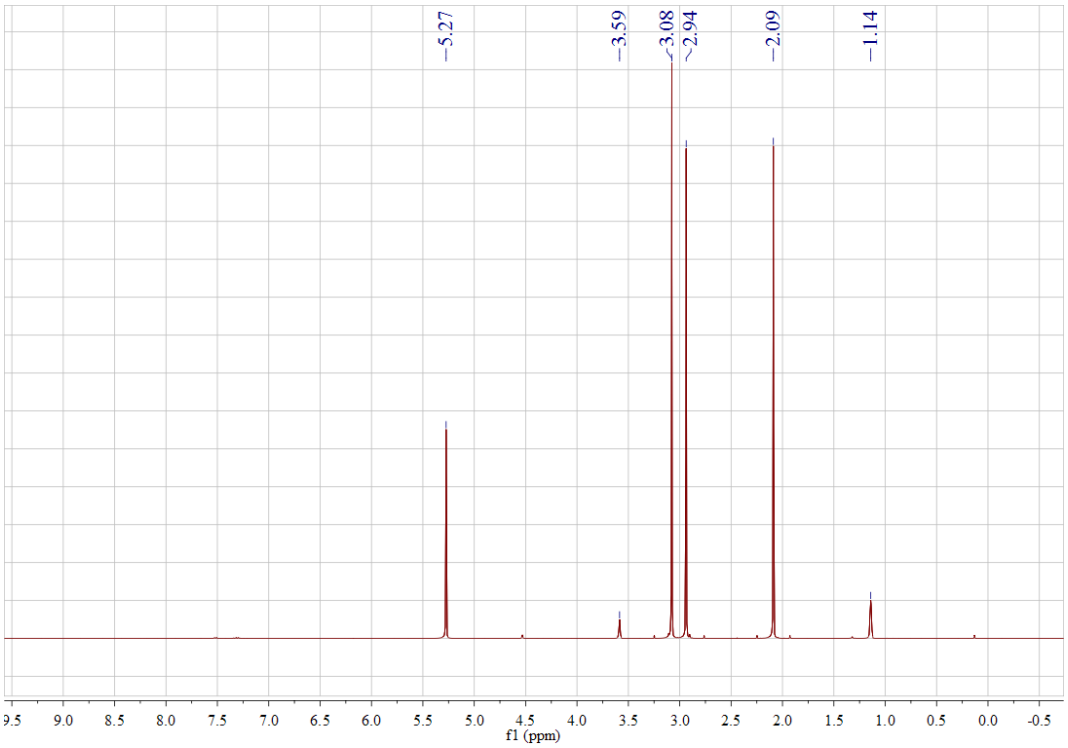

Figure S3. The ^{1}H NMR spectra of PhBr that is extracted from as-synthesized $[Zn_{1-x}Cu_x]_8L_8$ (x = 0.30) crystals obtained from PhBr (400 MHz, EtOD, 293 K). The peak of PhBr can't be observed in 8-7ppm, which indicated that no any PhBr was included.

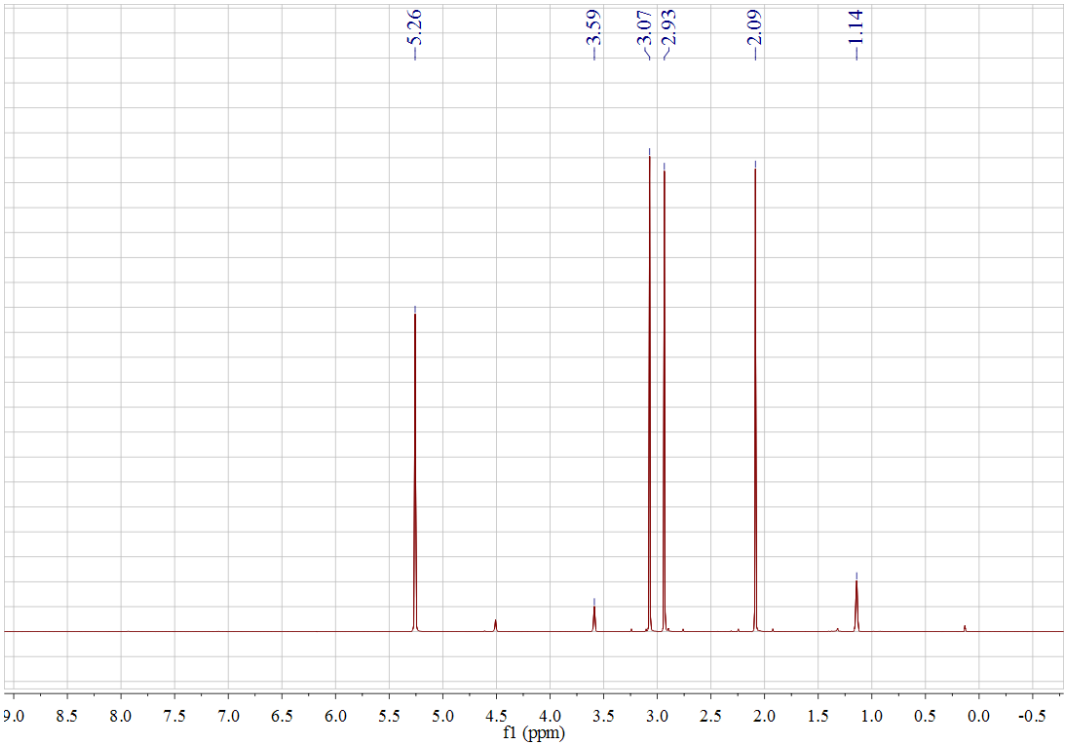

Figure S4. The ^{1}H NMR spectra of PhBr that is extracted from as-synthesized $[Zn_{1-x}Cu_x]_8L_8$ (x = 0.35) crystals obtained from PhBr (400 MHz, EtOD, 293 K).

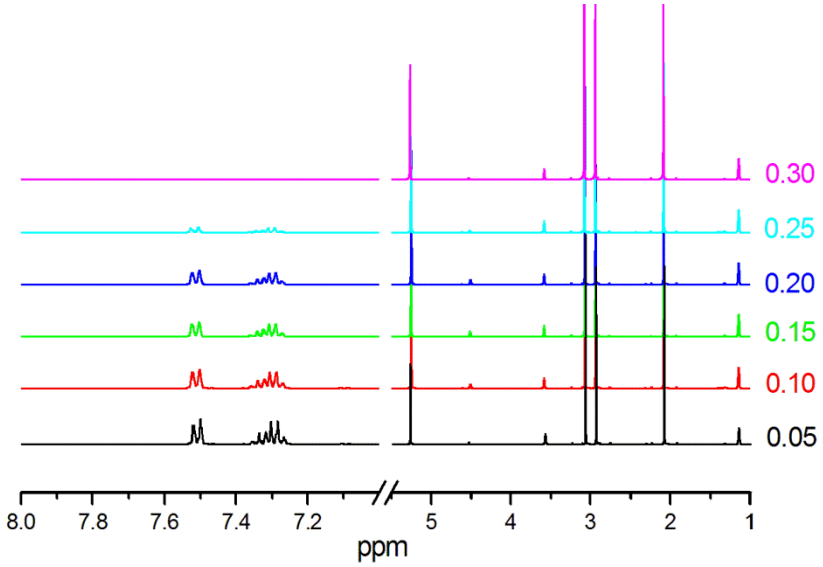

Figure S5. The ^{1}H NMR spectra of PhBr that is extracted from the same amount of as-synthesized $[Zn_{1-x}Cu_x]_8L_8$ (x = 0.05, 0.10, 0.15, 0.20, 0.25, 0.30) crystals obtained from PhBr by soaking in deuterated ethanol for 24 hours at room temperature.

4. High-resolution mass spectra

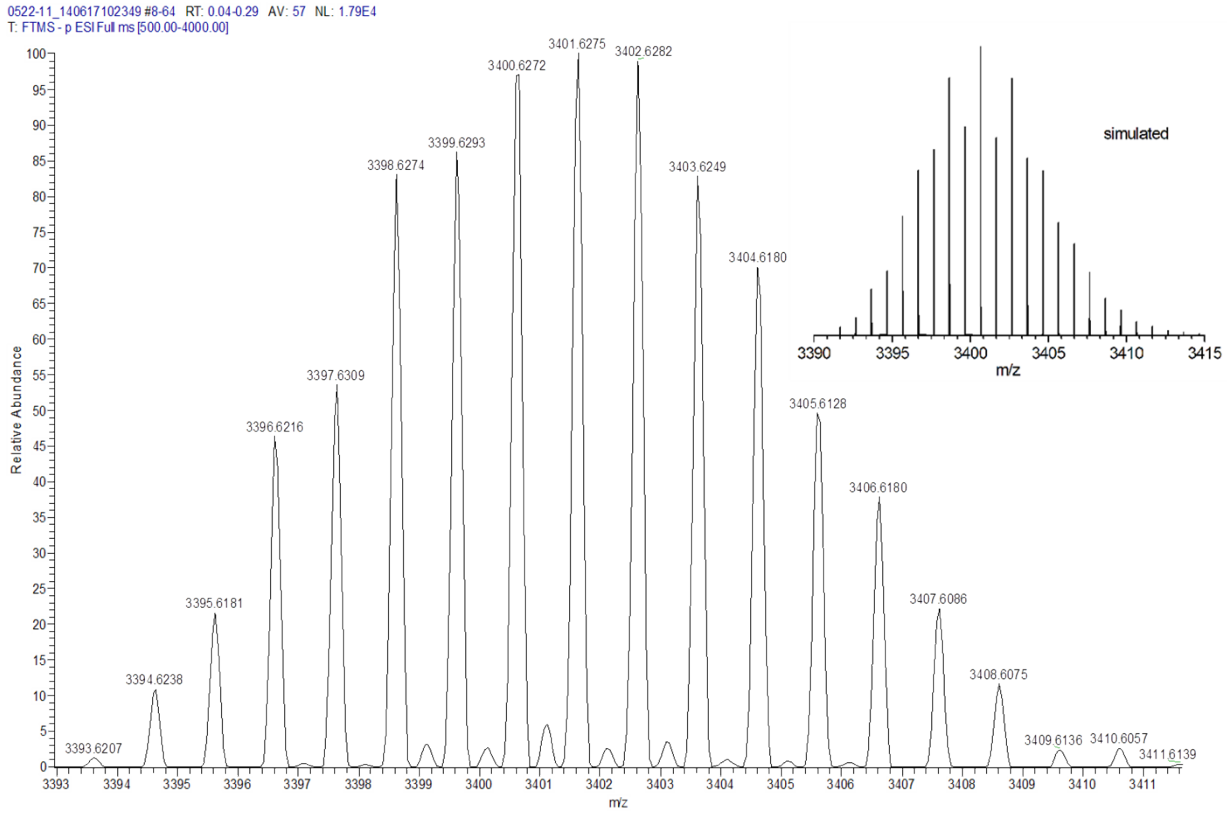

Figure S6. The High-resolution mass spectra for complex Cu_8L_8.

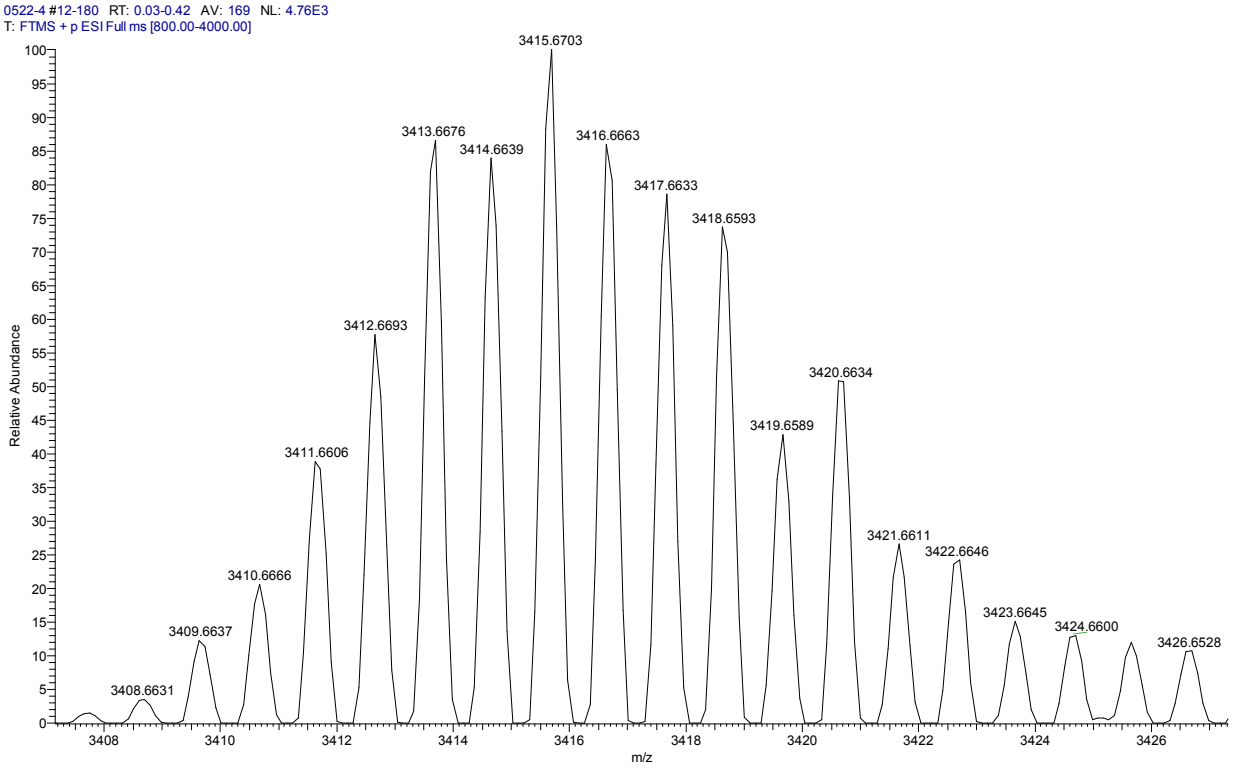

Figure S7. The High-resolution mass spectra for $[Zn_{1-x}Cu_x]_8L_8$ (x = 0.10) ($Zn_{7.22}Cu_{0.78}L_8$).

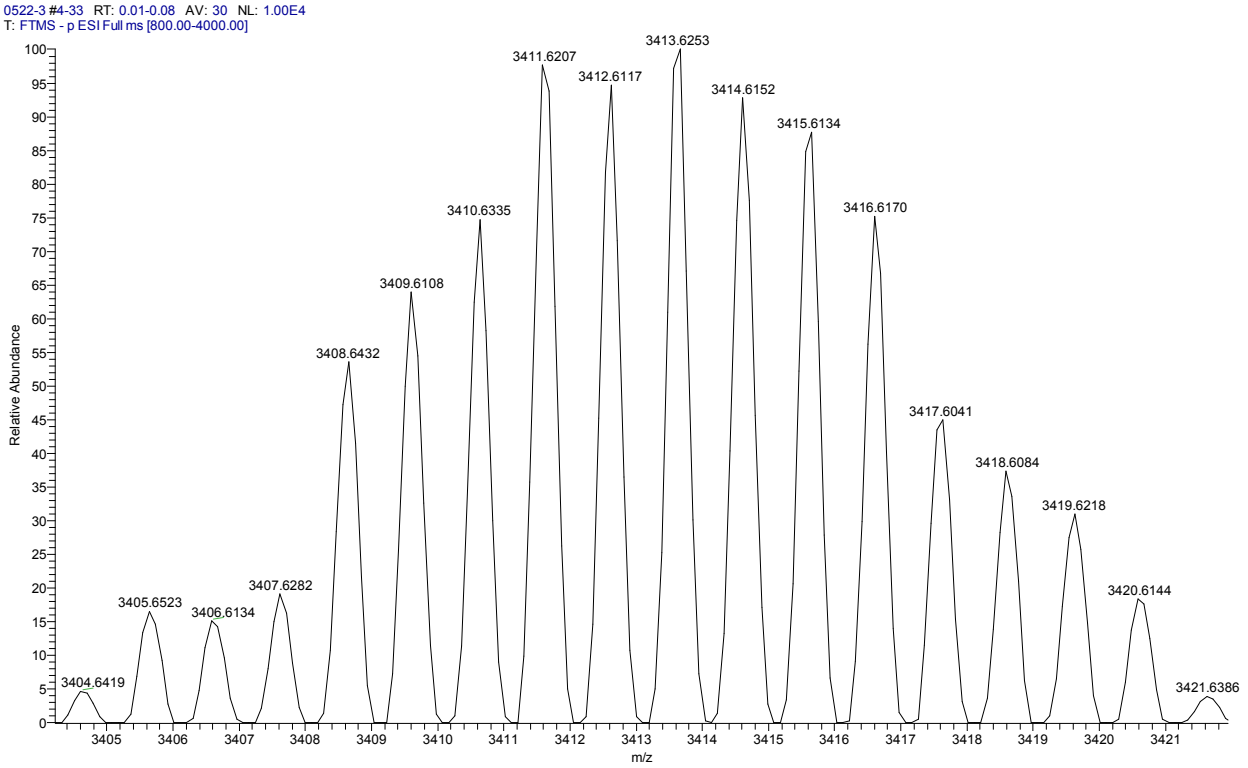

Figure S8. The High-resolution mass spectra for $[Zn_{1-x}Cu_x]_8L_8$ (x = 0.25) ($Zn_{6.00}Cu_{2.00}L_8$).

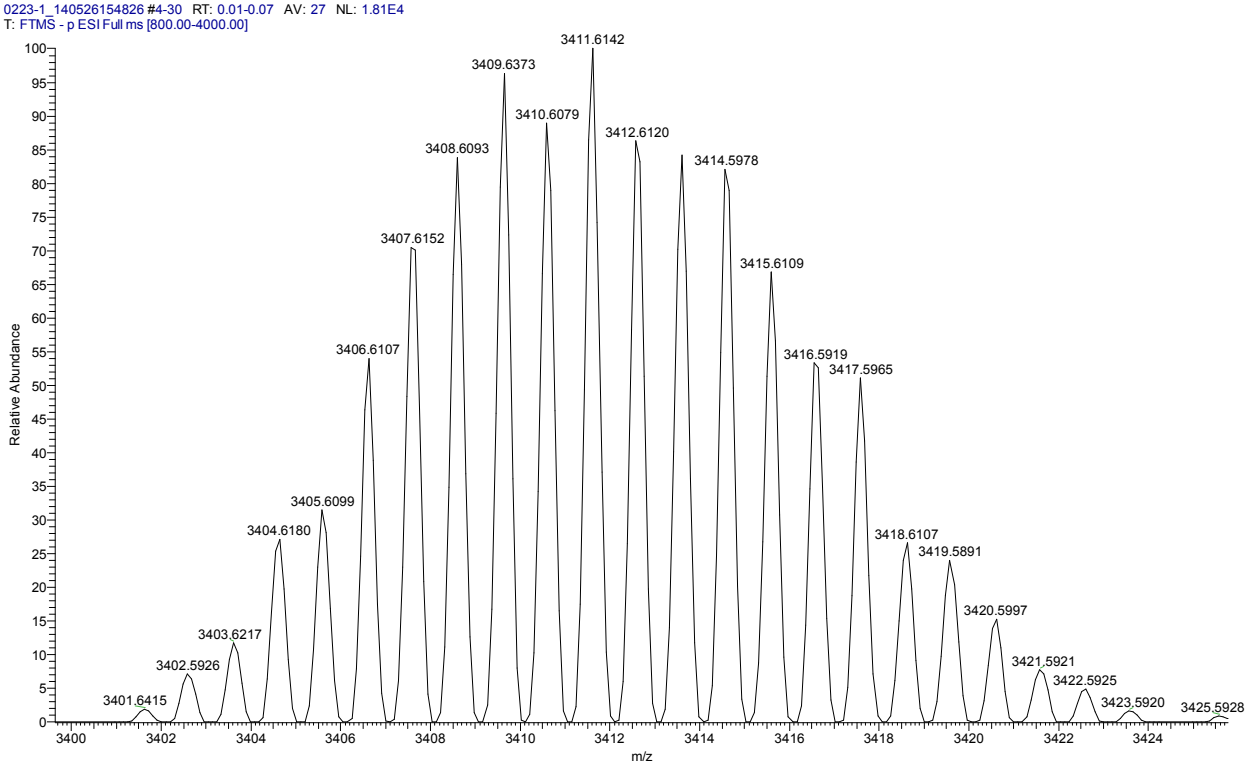

Figure S9. The High-resolution mass spectra for $[Zn_{1-x}Cu_x]_8L_8$ (x = 0.35) ($Zn_{4.84}Cu_{3.16}L_8$).

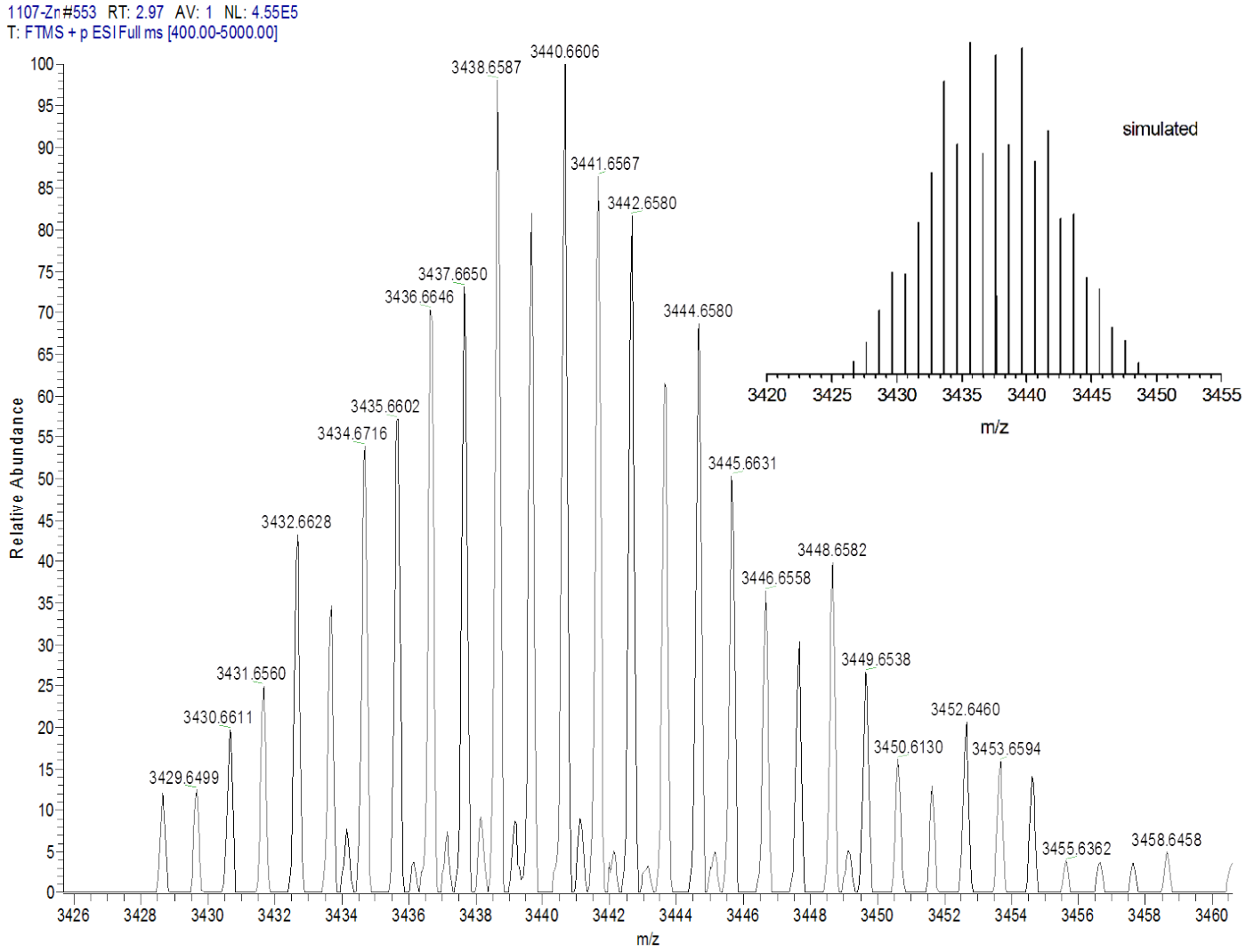

Figure S10. The High-resolution mass spectra for complex Zn_8L_8.

5. Elemental analyses

Table S8. Elemental analyses (ICP) for $[Zn_{1-x}Cu_x]_8L_8$ (x = 0.05, 0.10, 0.15, 0.20, 0.25, 0.30, 0.35)

Molar ratio of Cu:Zn	Wt% Cu Calcd (Found)	Wt% Zn Calcd (Found)
5%:95%	4.87 (4.75)	95.13 (95.25)
10%:90%	9.74 (9.44)	90.26 (90.56)
15%:85%	14.64 (14.78)	85.36 (85.22)
20%:80%	19.54 (19.73)	80.46 (80.27)
25%:75%	24.46 (24.44)	75.54 (75.56)
30%:70%	29.40 (30.12)	70.60 (69.88)
35%:65%	34.35 (38.75)	65.65 (61.25)

6. X-ray Powder Diffraction

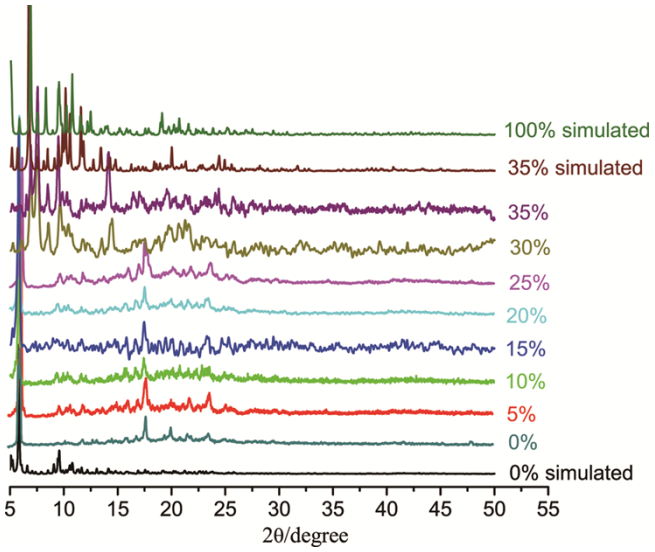

Figure S11: The recorded PXRD patterns of as-synthesized crystals $[Zn_{1-x}Cu_x]_8L_8$ (x = 0%, 5%, 10%, 15%, 20%, 25%, 30% and 35%) as well as the simulated patterns of $[Zn_{1-x}Cu_x]_8L_8$ (x = 0 %, 35% and 100%).

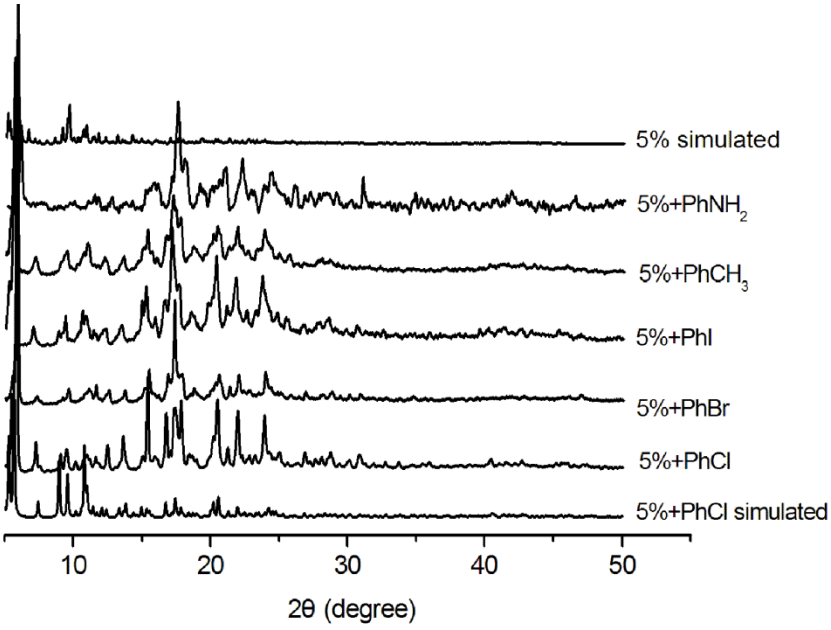

Figure S12. The recorded PXRD patterns of as-synthesized crystals $[Zn_{1-x}Cu_x]_8L_8$ (x = 5%) obtained from different guests.

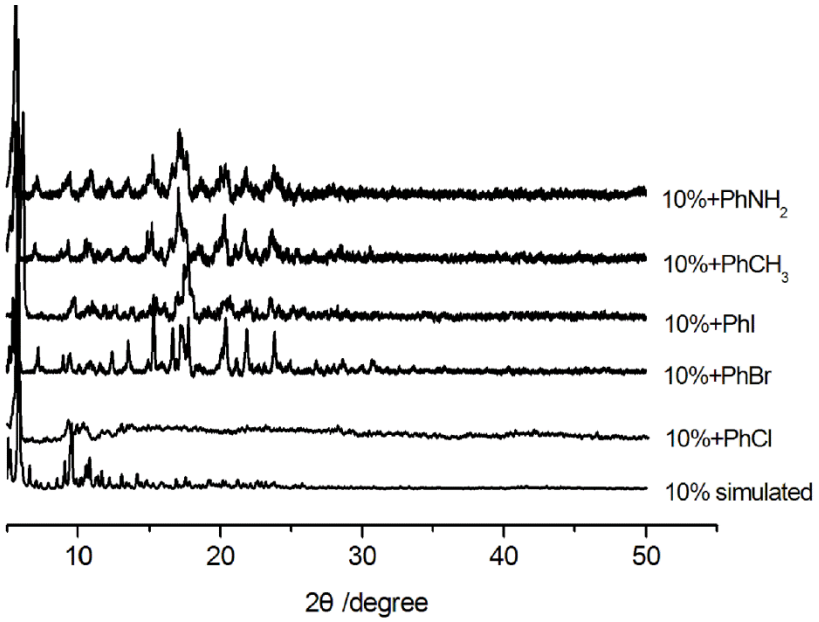

Figure S13. The recorded PXRD patterns of as-synthesized crystals $[Zn_{1-x}Cu_x]_8L_8$ (x = 10%) obtained from different guests.

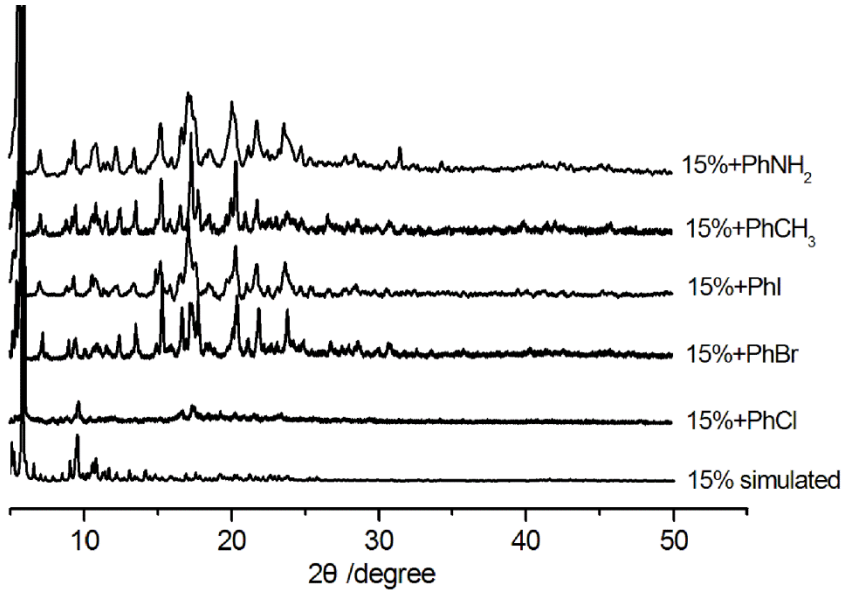

Figure S14. The recorded PXRD patterns of as-synthesized crystals $[Zn_{1-x}Cu_x]_8L_8$ (x = 15%) obtained from different guests.

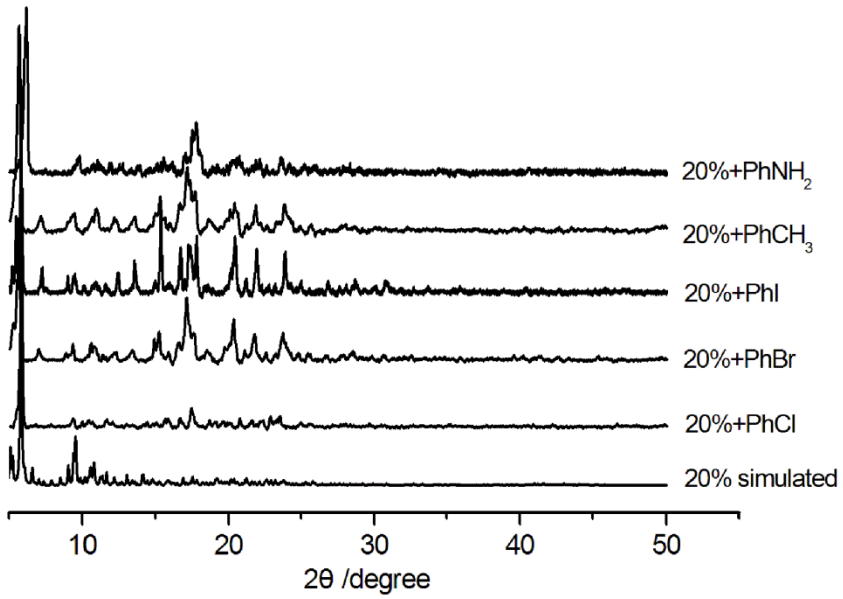

Figure S15. The recorded PXRD patterns of as-synthesized crystals $[Zn_{1-x}Cu_x]_8L_8$ (x = 20%) obtained from different guests.

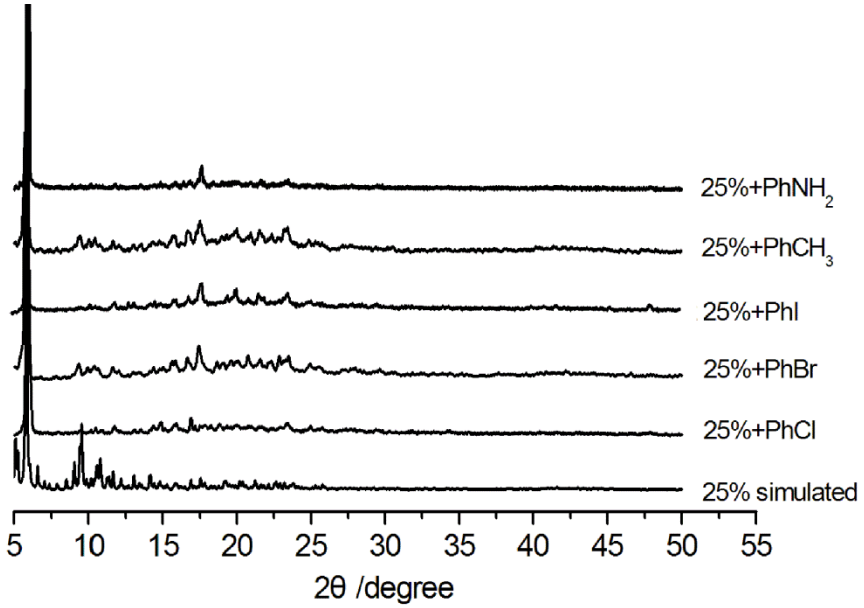

Figure S16. The recorded PXRD patterns of as-synthesized crystals $[Zn_{1-x}Cu_x]_8L_8$ (x = 25%) obtained from different guests.

7. Electrostatic Potential Calculation

Electrostatic Potential Calculation of complex Cu_8L_8 and open Zn_8L_8 were performed using the DFT hybrid functional B3LYP with the 6-31G** basis set as implemented in Gaussian03[S4]. The electrostatic potential was to the full range at isovalue of 0.001 electrons/Bohr^3 for the electron density and was visualized by a brainbow color ramp continuously from red-orange-yellow-green-cyan-blue (electron rich to electron poor).

8. References

[S1] Wang, X. C.; Li, Z.; Da, Y. X.; Chen, J. C. *Synth. Commun*. **2000**, *30*, 3405-3412.

[S2] Sheldrick. G. Acta Cryst. 2008, A64, 112-122.

[S3] Spek, A. L. *J. Appl. Cryst.* **2003,** *36*, 7-13.

[S4] M. J.Frisch, G. W. Trucks, H. B. Schlegel, G. E. Scuseria, M. A. Robb, J. R. Cheeseman, J. A. Montgomery Jr, T. Vreven, K. N. Kudin, J. C. Burant, J. M. Millam, S. S. Iyengar, J. Tomasi, V. Barone, B. Mennucci, M. Cossi, G. Scalmani, N. Rega, G. A. Petersson, H. Nakatsuji, M. Hada, M. Ehara, K. Toyota, R. Fukuda, J. Hasegawa, M. Ishida, T. Nakajima, Y. Honda, O. Kitao, H. Nakai, M. Klene, X. Li, J. E. Knox, H. P. Hratchian, J. B. Cross, V. Bakken, C. Adamo, J. Jaramillo, R. Gomperts, R. E. Stratmann, O. Yazyev, A. J. Austin, R. Cammi, C. Pomelli, J. W. Ochterski, P. Y. Ayala, K. Morokuma, G. A. Voth, P. Salvador, J. J. Dannenberg, V. G. Zakrzewski, S. Dapprich, A. D. Daniels, M. C. Strain, O. Farkas, D. K. Malick, A. D. Rabuck, K. Raghavachari, J. B. Foresman, J. V. Ortiz, Q. Cui, A. G. Baboul, S. Clifford, J. Cioslowski, B. B. Stefanov, G. Liu, A. Liashenko, P. Piskorz, I. Komaromi, R. L. Martin, D. J. Fox, T. Keith, M. A. Al-Laham, C. Y. Peng, A. Nanayakkara, M. Challacombe, P. M. W. Gill, B. Johnson, W. Chen, M. W. Wong, C. Gonzalez and J. A. Pople (2004) Gaussian 03, Gaussian Inc., Wallingford, CT.